Heliyon 9 (2023) e17944

Contents lists available at ScienceDirect

Heliyon

journal homepage: www.cell.com/heliyon

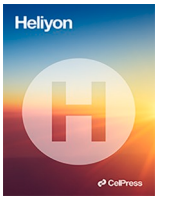

A theoretical study on the filtration efficiency and dust holding performance of pleated air filters

Bo Shi [a,b], Xinyi Yu [a,b], Yuan Pu [b], Dan Wang [a,b,*]

[a] State Key Laboratory of Organic-Inorganic Composites, Beijing University of Chemical Technology, Beijing 100029, China
[b] Research Center of the Ministry of Education for High Gravity Engineering and Technology, Beijing University of Chemical Technology, Beijing 100029, China

ARTICLE INFO

Keywords:
Pleated filter
Air purification
Numerical model
Particle filtration
Dust holding

ABSTRACT

Filter media composed of electrostatically charged nonwovens is the key device in an air purifier. Pleated filters are constructed from a cardboard frame with lattice faces containing a filter media reinforce by an expanded support grid, which have more surface area for trapping contaminants and capture airborne contaminants more effectively than non-pleated air filters. The aim of this work is to investigate the dominant factors on the filtration efficiency and dust holding performance of pleated filter by using a modified numerical model. It is found that geometric parameters of pleated filter play important roles to efficiency of the air purifier based on particle loading and filtration efficiency. The stable structural parameters include bending angle of pleated filter material in the range of 0~60° and the ratio of bending portion less than 0.5. Lower filling degree and shorter length of pleated filter unit exhibit similar stability of efficiency, indicating that the change of structural parameters has little effects on the filtration performance. The knowledge obtained in this work provides concrete reference for the design of high-performance air-cleaner element.

1. Introduction

Clean air is the basis of the people's livelihood and health protection [1,2]. Industrial production, transportation, human settlements and personal protection are increasingly demanding for air purification [3–5]. In traditional air purification products, the core component that filters particles such as bacteria and viruses are usually organic fiber material with porous structure [6,7]. Air purification filter materials made of charged melt-blown polypropylene microfibers are the key consumable to determine the level of air purification system [8]. Filtration efficiency and dust holding performance are two key standards to evaluate the filter materials, which are mainly affected by fiber dimension filling degree, filter material structure and some environmental factors [9,10]. When the filter materials are processed into air-cleaner element, pleats or folds are usually used to provide a larger filtration area than traditional flat filters by decreasing the amount of space between each layer of material and also allow more particles to be trapped in the filter, resulting in greater effectiveness and efficiency [11,12]. Along with the rapid development of nanoscience and nanotechnology [13–17], nanoparticles with smaller diameters and larger surface areas, are suspended for longer in the air in industry plant, and the development of removal technology for nanoparticles is of considerable significance [18]. Therefore, the scientific knowledge on the

* Corresponding author. State Key Laboratory of Organic-Inorganic Composites, Beijing University of Chemical Technology, Beijing 100029, China.
E-mail address: wangdan@mail.buct.edu.cn (D. Wang).

https://doi.org/10.1016/j.heliyon.2023.e17944
Received 5 April 2023; Received in revised form 27 June 2023; Accepted 3 July 2023
Available online 5 July 2023

nanoscale and microscale structural components of fiber materials and their interaction with the environment, as well as development of theoretical models for simulation, optimization and scale-up of air-cleaner element in nanometer to micrometer multiscale, is of immense significance [7,19,20]. Previously, to investigate the effect of dust loading on the optimal design of pleated filter, Feng et al. [21] calculated the flow field through the filter by solving the Navier-Stokes equation with the Detached Eddy Simulation - Spalart Allmaras turbulence model. Kim and co-workers [22] investigated the collection efficiency of pleated filter by using the system consisted of particle generation, particle measurement and airflow control zones, indicating that both pleat length and pleating ratio have influences on the collection efficiency of pleated filter.

In this work, systematic theoretical studies on the design of pleated air filters are report. A modified model is developed to calculate the filtration and dust holding performance of pleated filters based on numerical model simulation. The effects of air flow, thickness, total length, proportion of curved section and filling degree on the performance of the filter are studied.

2. Theory and model

2.1. Model assumptions

A model suitable for the filtration performance and dust holding capacity of pleated filter material is established. The basic assumptions are as follows:

- The spatial particle distribution is uniform and independent of time. The effect of spatial pressure drop on air flow velocity and particle distribution and whether the particulate is hydrophilic or lipophilic are ignored.
- The fiber layers are stacked in parallel. Assuming that the fiber distribution in the fiber medium is evenly distributed and the fiber diameter is uniform (equaling to the average fiber diameter). The pleated structure has no effect on the filtration efficiency of single fiber.
- The airflow direction is perpendicular to the vertical projection plane of pleated fiber filter material, and the effect of filter material structure on airflow direction is ignored.
- Due to the adsorption between dust particles and the spatial hindrance effect, short-term dust accumulation will not have a negative impact on the filtration efficiency of the filter material because there will not be a significant pressure difference in the short term. The dust accumulation has no effect on the filtration efficiency, so it is further assumed that the dust accumulation layer is evenly distributed in the thickness direction. The structure is similar to that of the fiber layer, and there is no bending section in the length direction.
- Various influencing factors act independently in filtration efficiency and average dust holding performance.
- The neutral line of the pleated filter material is on the center line of the pleated filter material along the thickness direction, which has no extrusion and tensile deformation. The fiber filling degree is distributed in proportion according to the thickness direction, and the thickness of each layer is regarded as 10 μm. The fiber filling degree at the neutral line is equal to the fiber filling degree of the flat filters on the neutral line.
- The Reynolds number of airflow through pleated filter material has no effect on filtration efficiency and average dust holding performance. The Reynolds number is calculated as $Re = \rho d_f v/\mu$, The air flow is based on the test standard of 3 m^3 air purifier, i.e. 3 m^3/h to 30 m^3/h (the surface velocity is about 0.1061 m/s to 1.0610 m/s, according to the flow surface radius of 5 cm), d_f is the fiber particle size (3 μm here), μ is the dynamic viscosity of air (15.7 μPa • s here). So the Reynolds number range is 0.0243–0.2433. It is smaller than 1, indicating tht the flows are in stokesflow region [23,24].

2.2. Single fiber efficiency

Since the pleated structure has no effect on the single fiber filtration efficiency, the single fiber filtration efficiency (E_T) can be calculated by eq (1) [25,26].

$$E_T = E_D + E_C + E_{DC} + E_I + E_G \tag{1}$$

Where E_D, E_C, E_I and E_G correspond to diffusion efficiency, collision interception efficiency, inertia and gravity capture efficiency respectively. E_{DC} is improved capture efficiency by particle diffusion which proposed by Hind [27].

Due to the small mass of particle, gravity capture efficiency (E_G) can be ignored. E_D, E_{DC}, E_C and E_I can be written as eqs (2)–(5) [24,27–30]

$$E_D = APe^m \tag{2}$$

$$E_{DC} = \frac{1.24R^{2/3}}{(Ku \times Pe)^{0.5}} \tag{3}$$

$$E_C = \frac{1+R}{2Ku}\left[2\ln(1+R) + \left(\frac{1}{1+R}\right)^2\left(1-\frac{\alpha_0}{2}\right) - \frac{\alpha_0}{2}(1+R)^2 + \alpha_0 - 1\right] \tag{4}$$

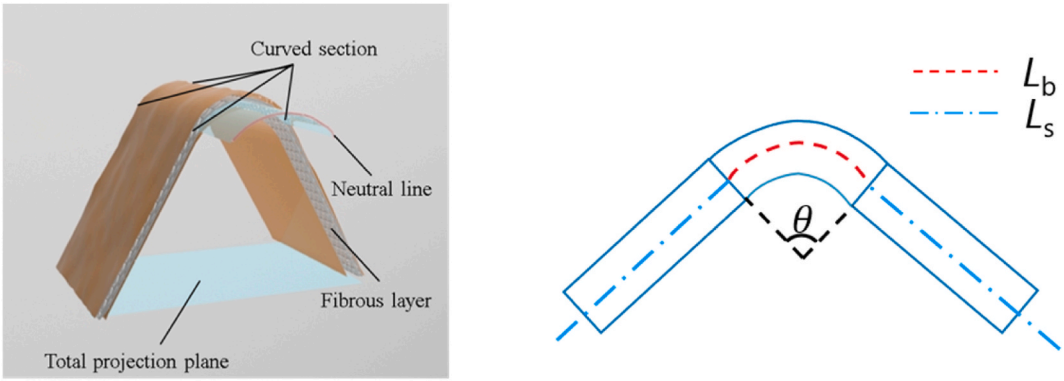

Fig. 1. Structural diagram of pleated filter material.

$$E_I = \frac{1}{(2Ku)^2}\left[\left(29.6 - 28{\alpha_0}^{0.62}\right)R^2 - 27.5R^{2.8}\right]Stk \tag{5}$$

Where α_0 is the filling degree of single fiber. As reported by Wang et al. [23], A and m are respectively taken as 0.87 and −0.41. *Pe*, *Ku*, *Stk* and *R* are three dimensionless numbers corresponding to Pelect number, Kuwabara hydrodynamic factor and particle size ratio respectively. The calculation method is given as eqs (6)–(9)

$$Pe = \frac{d_f v}{kTB} \tag{6}$$

$$Ku = -\frac{\ln \alpha_0}{2} - \frac{{\alpha_0}^2}{4} + \alpha_0 - \frac{3}{4} \tag{7}$$

$$Stk = \frac{\rho_p {d_p}^2 C_c v}{18\mu d_f} \tag{8}$$

$$R = \frac{d_p}{d_f} \tag{9}$$

Where d_f (fiber diameter) is taken as 3 μm and d_p (particle size) is taken as 0.1 μm. The ρ_p (particle density) is taken NaCl as reference, which is given as 2165 kg/m^3. The *k* is Boltzmann constant and *T* is temperature (300 K here). The particle mechanical mobility (*B*) and Cunningham sliding correction factor (C_c) [23] are given as eq (10) and eq (11)

$$B = \frac{C_c}{3\pi\mu d_p} \tag{10}$$

$$C_c = 1 + \frac{\lambda}{d_p}\left[2.34 + 1.05e^{\left(-0.39d_p/\lambda\right)}\right] \tag{11}$$

2.3. Pleated filter material efficiency

According to hypothesis 2, the pleated structure has no effect on the filtration efficiency of single fiber. It can be seen that the filling degree of single fiber remains invariant. Therefore, the filtration efficiency of pleated structure filter material can be expressed as eq (12) [31].

$$E_m = 1 - P_m = 1 - e^{\left(-4\alpha E_T Z/\pi d_f(1-\alpha)\right)} \tag{12}$$

As reported by Zhao et al. [32], the filtration efficiency of the electret filter material is given as eq 13

$$E_e = 1 - (1 - E_m)\left(\frac{d_p}{d_c}\right)^{-K_c\sigma[1-\ln(v)]} \tag{13}$$

Where E_e is electrostatic filtration efficiency, σ is fiber electrization strength. Critical particle size of electrostatic effect (d_c) [33] and K_c [31] is constant, which are taken as 20 nm and 2664.3 respectively.

According to hypothesis 6, at the bending section of pleated filter material, its relationship with vertical distance (α_d) is given as eq (14)

$$\alpha_d = \frac{\alpha l}{\left(\theta \times \left(\frac{l}{\theta} + \frac{Z}{2} - d_l\right)\right)} \tag{14}$$

Where Z is the total thickness of filter material, α is fiber filling degree of fiber layer of 10 μm, θ is the bending angle of pleated filter material, l is the length of neutral line at the bending section, d_l is the distance to the outermost side of the bending section, as shown in Fig. 1.

The electrostatic filtration efficiency of each layer of fiber in the bending section can be calculated with formula (14). According to the definition of fiber filtration efficiency, it is obvious to obtain the total filtration efficiency of the bending section, as shown in the eq (15)

$$E_{eb} = 1 - \frac{N_d}{N_u} = 1 - \frac{N_{d,n-1}P_{e,n}}{N_u} = 1 - P_{e,1}P_{e,2}\cdots P_{e,n} \tag{15}$$

The filtration outside the curved section of the filter material is ignored, so the equivalent filtration efficiency (η) of the pleated filter material is defined as eq 16

$$\eta = \frac{E_e \times L_s + E_{eb} \times L_b}{E_e \times L} \tag{16}$$

Where L is the total length of pleated fiber filter material, L_s is the total projection length of straight edge of pleated fiber filter material, L_b is the total projected length of the bending section. The geometric effect of filter material thickness is ignored in calculation of η.

2.4. Dust holding capacity of pleated filter material

The experimental test standard for the dust capacity of general filter materials is the dust capacity of filter materials when the initial resistance is twice. According to the national standard of China for air cleaner (GB/T 18801-2015), the air purifier is divided into two test standards by volume, in which the air flow of 30–300 m^3/h corresponds to the air purifier of 30 m^3, and the air flow of 3-30 m^3/h corresponds to the air purifier of 3 m^3. In this work, the test standard corresponding to 3 m^3 air purifier is selected for calculation. In order to simplify the calculation, the average dust holding performance of pleated filter material is defined as eq (17)

$$K = \frac{\left(P^{End}_{Pleated}/P^{Origin}_{Pleated}\right)}{\left(P^{End}_{Tile}/P^{Origin}_{Tile}\right)} \tag{17}$$

Saleh et al. [34] obtained the dust accumulation of rectangular filter material through mass conservation and Darcy's theorem. By taken it as a reference, a calculation method suitable for pleated filter material is established through appropriate approximation and assumptions. According to Darcy's definite reason, the pressure drop is given as eq (18) [24,35].

$$P = v \times r = v \times C_d \frac{4\mu\alpha Z}{\pi d^2} \tag{18}$$

Where d is the average diameter of the dust layer and the fiber layer, C_d is the resistance coefficient. Since the density of the dust layer is much smaller than that of the fiber layer, the particle size is small and the dust is easy to agglomerate. At the same time, according to Hypothesis 4, the dust layer has no effect on the filtration efficiency of the filter material, d can be approximately taken as the fiber diameter. C_d and αZ can be calculated by the eq (19) and eq (20), where C_d can be approximately calculated according to the maximum resistance coefficient (i.e. the resistance coefficient of the fiber layer)

$$C_d = 4\pi\alpha^{0.5}\left(1 + 56\alpha^3\right) \tag{19}$$

$$\alpha Z_{total} = \alpha_p Z_{dust} + \alpha Z \tag{20}$$

Where α_p is the filling degree of the dust layer. Since the minimum fiber filling degree is 0.1, it is advisable to set the filling degree of the dust layer to 0.1 to simplify the calculation according to hypothesis 4.

According to the conservation of mass, the velocity v is calculated as eq (21)

$$u = \frac{v \times L \times \sin\left(\frac{\theta}{2}\right)}{\left(L \times \sin\left(\frac{\theta}{2}\right) \times \left(1 - 4 \times \frac{h}{L}\right)\right)} \tag{21}$$

Here, the pressure drop of the flat filter material has been calculated, and the bending angle of the pleated filter material needs to be considered. The pressure drop can be approximately calculated as eq (22)

$$\Delta p = v \times \left(r_1\left(\frac{L \times \cos\left(\frac{\theta}{2}\right)}{L_s + L_b}\right) + r_2\left(1 - \frac{L \times \cos\left(\frac{\theta}{2}\right)}{L_s + L_b}\right)\right) \tag{22}$$

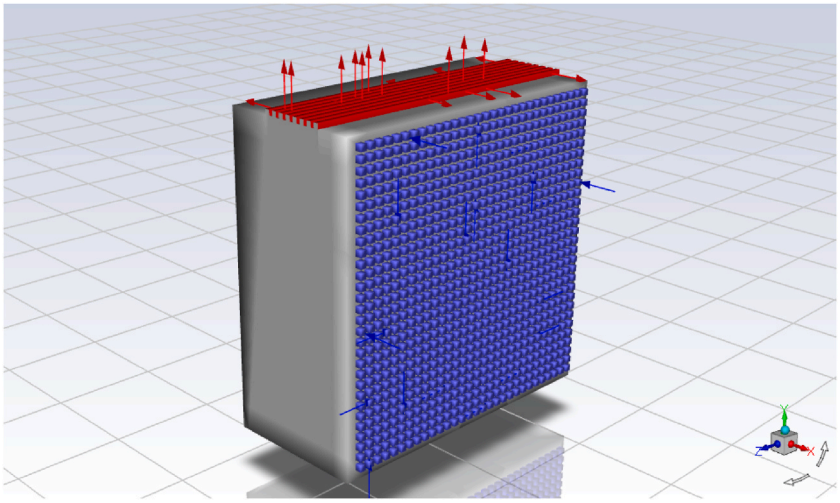

Fig. 2. Diagram of the miniature air purifier in hydrodynamic simulation.

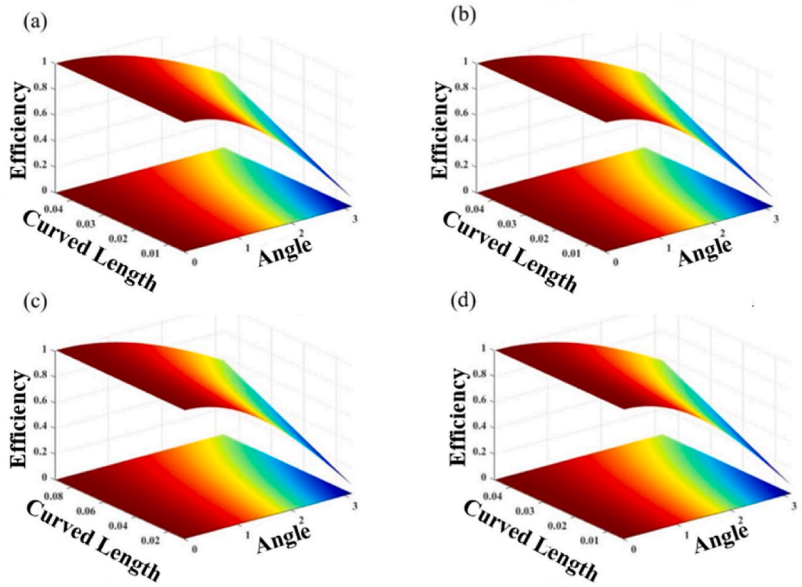

Fig. 3. Filtration efficiency of pleated filter material at 3 m^3/h and 0.2 fill rate (a 1 mm thick, 5 cm total length), at 30 m^3/h and 0.2 fill rate (b 2 mm thick, 5 cm total length; c 1 mm thick, 10 cm total length), at 30 m^3/h and 0.6 fill rate (d 2 mm thick, 10 cm total length).

r_1 is the contribution of pressure drop on the projection plane perpendicular to the air flow direction. r_2 is the contribution of pressure drop parallel to the projection plane of the air flow direction

2.5. Hydrodynamic simulation of miniature air purifier

In this paper, the discrete phase treatment of dusty air is carried out by using porous media model through fluent simulation software. The inertial resistance and viscous resistance are converted by the eq (23) and eq (24) [36].

$$C = \frac{0.54388}{\rho \Delta n} \tag{23}$$

$$D = \frac{1}{\alpha} = \frac{4.85211}{\mu \Delta n} \tag{24}$$

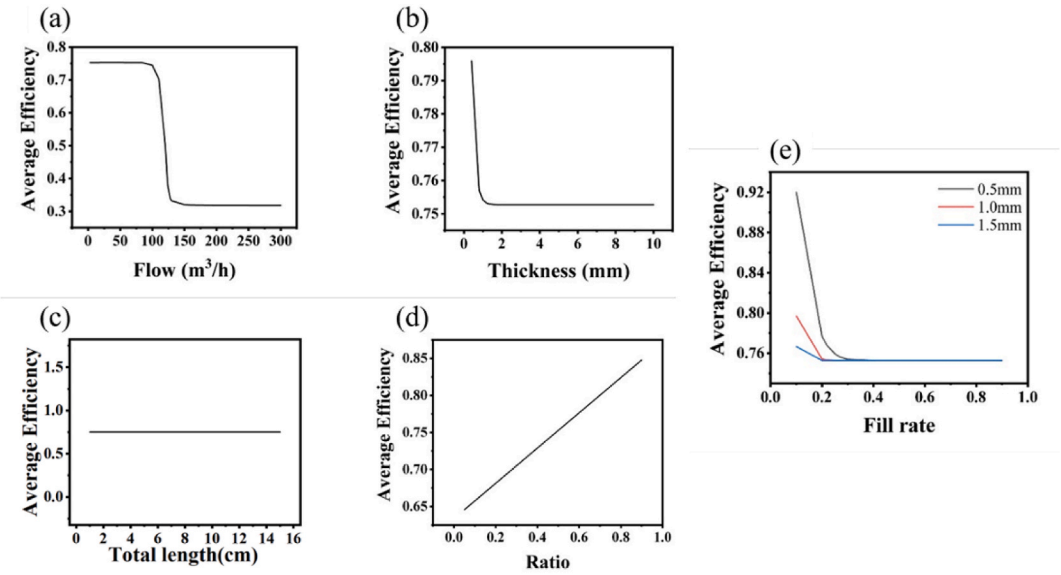

Fig. 4. Effect of flow rate (a) and thickness (b) on average filtration efficiency at 5 cm total length, 0.5 proportion of curved section and 0.2 fill rate; Effect of flow rate (c) and thickness (d) on average filtration efficiency at 15 m^3/h, 2 mm thickness and 0.2 fill rate; Effect of flow fill rate (e) on average filtration efficiency at 15 m^3/h, 5 cm total length and 0.5 proportion of curved section.

C is inertial resistance. D is viscous resistance. Δn is the thickness of filter layer. ρ and μ is density and dynamic viscosity of air.

The model of air purifier is shown in Fig. 2. The whole model is based on the gravity field in - Y direction using transient simulation. The particle jet source is the surface normal jet, and the jet surface is the inlet surface. The viscosity model is SST k-omega. The air inlet is grid, the outlet is strip. The type of inlet boundary condition is velocity-inlet (0.5305 m/s), and the out boundary condition type is pressure-outlet (0 MPa, gage pressure).

3. Results and discussion

3.1. Effect of various parameters on efficiency

According to the assumptions and formulas in section 2, the filtration efficiency of filter material at 3 m^3/h and 30 m^3/h gas velocity associated with the angle (θ) of pleated filter material (1/180 to π) and curved length are obtained (Fig. 3), in which the curved section accounts for 1/10 to 9/10 of the total length. In Fig. 3(a–d) it is observed that the smaller the degree of bending, the higher filtration efficiency would achieved, while the proportion of curved section has less effect on the filtration efficiency. With the increase of angle, the filtration efficiency gradually decreases. Increasing the length of the curved section can slow down the downward trend. Generally, by compare Fig. 3 (a) with Fig. 3(b–d) the filtration efficiency of the filter material is little affected by the total length, thickness and air flow. However, with the increase of the filling degree, the filtration efficiency of the filter material generally decreases to a certain extent. Under the appropriate angle and the length of the curved section, the filtration efficiency of the pleated filter material is even greater than that tiled according to the total number of effective filter particles.

Furthermore, keeping the condition of other parameters constant, the effect of a single parameter on filtration efficiency have been obtained respectively, as shown in Fig. 4 below. Fig. 4(a) shows the change of the average efficiency of 2 mm filter material at the gas volume of 1 m^3/h to 300 m^3/h. It can be perceived that there are three different gas velocity regions. The average efficiency in the low velocity region (Re from 0.0243 to 0.6812) remains constant. This is because the pelect number and Stokes number are less affected in the low-speed zone, which has little impact on the diffusion interception efficiency and inertial interception efficiency. In practical application, low gas velocity corresponds to low load operation. At this time, the average filtration efficiency of pleated filter material (based on the total number of effective particle filtration) is almost the same as that of tiled filter material. In the transition zone (Re from 0.6812 to 1.2165) The average efficiency decreases rapidly because Reynolds number transits near 1 and pelect number and Stokes number change greatly. In practical application, the working load in the transition zone will change greatly between low load and high load. In the high velocity zone (re from 1.2165 to 2.4329) the average efficiency of pleated filter material is low, so it is more suitable to adopt tiled structure. Fig. 4 (b) shows the change of average efficiency when the air volume is 15 m^3/h and the thickness of filter material is from 1 mm to 10 mm. It can be perceived that when the thickness is large, the filtration efficiency of pleated filter material is low and remains constant. Since the filtration performance improves with the increase of thickness, the advantage derived from curved section of pleated filter material in improving fiber dimension filling decreases. Meanwhile when the thickness reaches a certain value, the filtration performance cannot be improved. It is worth mentioning that the filtration efficiency discussed here is based on the total number of effective particle filtration, so a value less than 1 does not fully mean that the filtration performance of

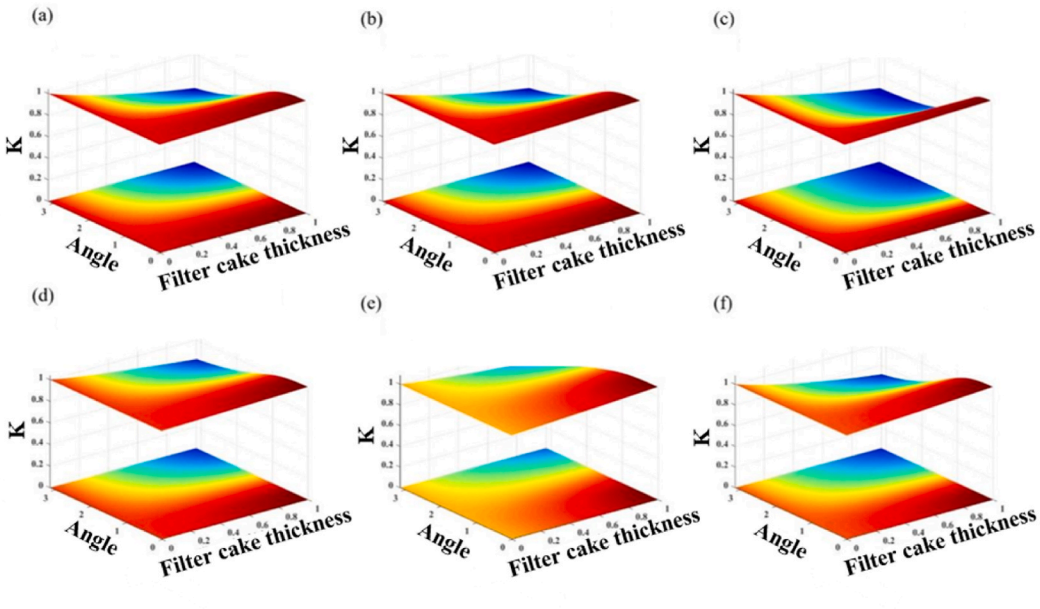

Fig. 5. Average dust holding performance of pleated filter material at two kinds of fill rate and total length: 0.2 fill rate (a 3 m^3/h, 1 mm thickness and 0.1 propotion of bending; b 30 m^3/h, 1 mm thickness and 0.1 propotion of bending; c 30 m^3/h, 1 mm thickness and 0.5 propotion of bending), 0.4 fill rate (d 30 m^3/h, 1 mm thickness and 0.3 propotion of bending,; e 30 m^3/h, 1 mm thickness and 0.1 propotion of bending; f 30 m^3/h, 0.05 mm thickness and 0.1 propotion of bending); 10 cm total length (a,b,c,d), 5 cm total length (e,f).

pleated filter material is inferior to that of tiled filter material. Fig. 4 (c) presents the change of average efficiency when the proportion of bending section is 0.5 and the total length is from 1 cm to 15 cm. Obviously, the average filtration efficiency of pleated filter material is not a function of the total length. In practical application, when the fiber material of filter material, the fiber filling degree and the bending angle is certain, increasing or decreasing the fiber length will not affect the total number of effective particle filtration in the corresponding space. Fig. 4 (d) shows the average efficiency when the total length is 5 cm and the proportion of bending section ranges from 0.1 to 0.9. The relationship between the two presents a first-order function and increases monotonically. This is because the larger proportion of bending section corresponds to more parts of fiber filling enhancement. Fig. 4(e) calculates the effect of filling degree on average efficiency under three different kinds of thicknesses. When the thickness is 0.5 mm and the fiber packing density is below 0.3, the pleated filter material can maintain a significant advantage, and the average filtration efficiency can reach about 0.92. When the thickness is greater than about 1 mm, the average filtration efficiency decreases significantly, dropping below 0.8. As the fiber packing density increases, the advantages brought by the pleated structure become less obvious. When the fiber packing density reaches 0.2, the advantages almost disappear.

When the thickness and fiber filling degree are low, the filtration efficiency of pleated filter material is at a bit high level. This is because the bending section enhances the filling degree more obviously when the fiber filling degree is low. However, the enhancement and the efficiency decreases with the increase of fiber filling degree. When the filling degree is large enough to reach the point that the filtration performance of flat filter material and pleated filter material reaches the maximum, the filtration efficiency of pleated filter material remains constant. With the increase of thickness, the effect caused by fiber filling degree decreases.

3.2. Effect of various parameters on average dust holding performance

It should be pointed out that K is obtained from eq (17), which indicates that the value of K is in inverse proportion to the average dust holding performance. By comparing Fig. 5(a) with Fig. 5(b–f), it is similar to the filtration efficiency that the air flow has little effect on the average dust holding performance. However, the effects of fiber filling degree, filter material thickness and the proportion of bending section are more obvious. It can be seen from Fig. 5 (b) and Fig. 5 (c) that with the decrease of the proportion of curved section the low average dust holding performance area decreases and the high average dust holding performance area expands obviously in terms of the effect of filter cake thickness. In terms of the effect of angle, the low average dust holding performance area and medium average dust holding performance area are almost unchanged. Obviously, the arc structure has stronger compressive performance, so its average dust holding performance is correspondingly higher. Since assumption 4 ignores the change of spatial pressure drop, the average dust holding performance area under the effect of angle keep almost unchanged. Fig. 5 (b) and Fig. 5 (d) show that the average dust holding performance decreases obviously as the filling degree increases, mainly in the overall increase the value of K in the high average dust holding performance area. However, the range of low average dust holding performance area remains almost unchanged. Fig. 5(e) and Fig. 5 (f) show that the reduction of total length will lead to a significant decrease in average dust holding performance. But at the same time, reducing the thickness can slow down the impact.

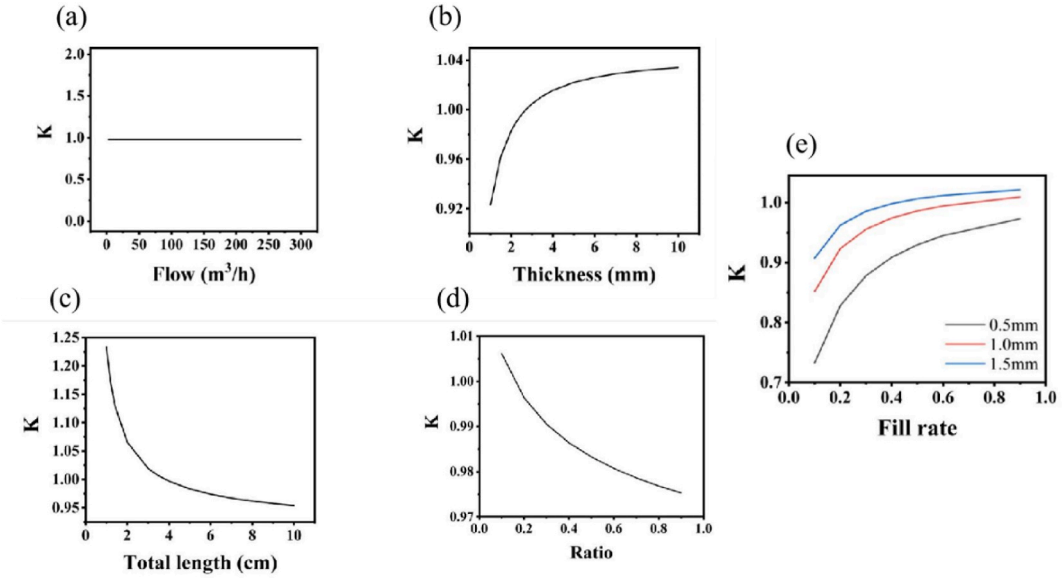

Fig. 6. Effect of flow rate (a) and thickness (b) on average dust holding performance at 5 cm total length, 0.5 proportion of curved section and 0.2 fill rate; Effect of flow rate (c) and thickness (d) on average dust holding performance at 15 m^3/h, 2 mm thickness and 0.2 fill rate; Effect of flow fill rate (e) on average dust holding performance at 15 m^3/h, 5 cm total length and 0.5 proportion of curved section.

In addition, keeping the condition of other parameters constant, the effect of a single parameter on average dust holding performance have been obtained respectively. Fig. 6(a) shows the change of average dust holding performance when the thickness is 2 mm and the flow is from 1 m^3/h to 300 m^3/h. It indicates that the average dust holding performance is not a function of air flow. Since the filter material structure has not been changed, and it's value of *K* is calculated by pleated filter material and tiled filter material under the same working conditions, which does not change in essence. Meanwhile, the figure shows that the value of *K* is close to but less than 1. Fig. 6(b) shows the change of average dust holding performance under the air flow of 15 m^3/h and the thickness from 1 mm to 10 mm. Generally, the average dust holding performance decreases monotonically with the thickness. When the thickness is low, the average dust holding performance decreases rapidly. When the thickness reaches about 3 mm, the average dust holding performance of pleated filter material is almost the same as that of tiled filter material. After the thickness of filter material exceeds 3 mm, the average dust holding performance of flat filter material is better than that of pleated filter material. Compared with the flat filter material, the average dust holding performance of the pleated filter material decreased by about 4%. Because the resistance will increase significantly under effect of the enhancement of fiber filling rate caused by bending section of pleated filter material and the increase of thickness. Thus, the bent section will produce greater air flow resistance, weakening the advantages of the pleated structure itself, resulting in a certain decrease in average dust holding performance. However, due to the advantages brought by the arc structure of pleated filter material, the increase of thickness will not cause too much loss of average dust holding performance. Fig. 6 (c) shows the change of dust holding performance when the proportion of curved section is 0.5, and the total length is from 1 cm to 10 cm. In the figure, *K* decreases with the total length, and the line type is similar to the inverse proportional function. The pleated filter material with lower total length corresponds to smaller spacing and volume, which is easier to be filled, resulting in a significant increase in resistance. With the increase of total length, the spacing and volume also increase. And due to the advantages of arc structure, the dust holding performance of pleated filter material is even better than that of flat filter material. Fig. 6 (d) shows the change of dust holding performance with a total length of 5 cm and the proportion of curved section from 0.1 to 0.9. Similar to Fig. 6 (c), it decreases monotonically in general, but the curve trend is more gentle in Fig. 6 (d). The increase of the proportion of curved section will increase the range of arc structure, to improve the dust holding performance. At low proportion, the dust holding performance is worse than that of tiled filter material. Because the low proportion lead to small spacing, which makes it easier to fill, increasing the resistance. Fig. 6 (e) calculates the influence of filling degree on dust holding performance under three different thicknesses. When the fiber packing density is less than 0.4, the dust holding capacity of the filter material increases rapidly with the increase of the packing density. At a fiber packing density of 0.1, the pleated filter material with a thickness of 0.5 mm has a relatively poor relative dust holding performance of about 0.74. When the thickness is 1.5 mm, it can reach about 0.91. The increase in dust holding performance of the 1.5 mm thick pleated filter material relative to the 1 mm thick pleated filter material is about 2 times the increase in dust holding performance of the 1 mm thick pleated filter material relative to the 0.5 mm thick pleated filter material. Under the same thickness, the dust holding performance decreases with the increase of filling degree, which is almost the same as the influence of thickness. The reason for this change is the same as that in Fig. 6 (b). The increase of filling degree increases the resistance. At high filling degree, the rise rate of *K* decreases. Because the bending section can enhance the filling degree. When the filling degree is small, the enhancement is obvious. With the increase of filling degree, the enhancement decreases gradually, thus *K* tends to be flat.

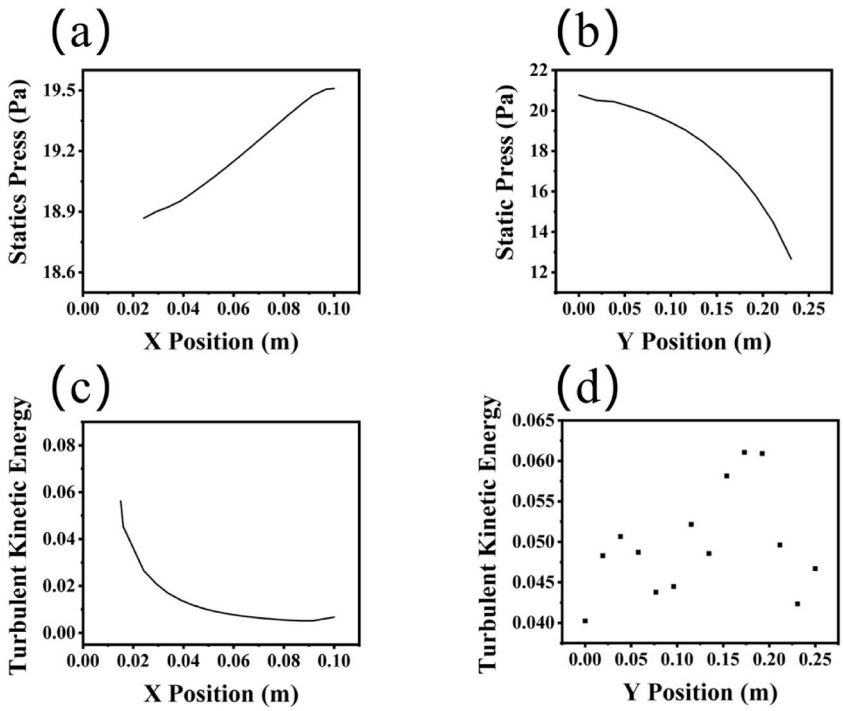

Fig. 7. Variation of static pressure and turbulent kinetic energy in X direction at center of Y-Z plane (a and c) and in Y direction at the center inside the filter zone (b and d).

3.3. Results of hydrodynamic simulation

Variation of static pressure and turbulent kinetic energy of miniature air purifier is represented in Fig. 7. In the width direction, after the air flows into the purifier from the inlet, the pressure drops by 0.6 Pa and the turbulent energy also decreases by about 30%. In the height direction, the pressure near the outlet is about 8 Pa lower than that at the inlet, while the turbulent energy shows disorderliness, roughly showing a trend of increasing, decreasing, increasing and finally decreasing. It can be seen from Fig. 7 (a) that the static pressure energy increases as X goes u. Because there is a certain resistance to the fluid in the filter screen area, so as to achieve the purpose of intercepting particles. In Fig. 7(b), in the filter screen area, the static pressure energy decreases with the increase of Y, which is the result of the gravity of the particles, so that the particles can be better trapped in the lower layer of the air purifier without being brought out of the air purifier. Fig. 7(c) shows the turbulent kinetic energy in the X direction. The turbulent kinetic energy reaches the maximum in the filter screen area, and then decreases rapidly until it tends to remain unchanged. This shows that the fluid mass transfer effect decreases, further showing the particle interception effect in the filter screen area. Fig. 7(d) shows the turbulent kinetic energy in Y direction in the filter screen area. It can be seen that the turbulent kinetic energy in the filter screen area is unevenly distributed, while the overall value is small. The flow situation is complex in filter screen area, but the mass transfer is poor and slow.

5. Conclusions

In summary, by comparing the tiled filter material, the influence of structural parameters on the filtration efficiency and dust holding performance of pleated filter material are systematic studied. In terms of filtration efficiency, the filtration efficiency as a function of bending section angle and initial length almost does not change with other parameters. The efficiency is not affected by the thickness, but the pleated filter material can show better filtration performance at low thickness. The stable structural parameters include bending angle of pleated filter material in the range of 0~60° and the ratio of bending portion less than 0.5. Lower filling degree and shorter length of pleated filter unit exhibit similar stability of efficiency, indicating that the change of structural parameters has little effects on the filtration performance. The knowledge obtained in this work provides concrete reference for the design of high-performance air-cleaner element.

Declaration of competing interest

The authors declare that they have no known competing financial interests or personal relationships that could have appeared to influence the work reported in this paper.

Acknowledgements

The authors are grateful for financial support from the Fundamental Research Funds for the Central Universities of China (buctrc202016).

References

[1] X. Lu, S. Zhang, J. Xing, Y. Wang, W. Chen, D. Ding, Y. Wu, S. Wang, L. Duan, J. Hao, Progress of air pollution control in China and its challenges and opportunities in the ecological civilization era, Engineering 6 (2020) 1423–1431.
[2] S. Dubey, H. Rohra, A. Taneja, Assessing effectiveness of air purifiers (HEPA) for controlling indoor particulate pollution, Heliyon 7 (2021), e07976.
[3] J. Patel, F. McGain, T. Bhatelia, S. Wang, B. Sun, J. Monty, V. Pareek, Vented individual patient (VIP) hoods for the control of infectious airborne diseases in healthcare facilities, Engineering 15 (2022) 126–132.
[4] S. Janhall, Review on urban vegetation and particle air pollution - deposition and dispersion, Atmos. Environ. 105 (2015) 130–137.
[5] M. Pena-Castro, M. Montero-Acosta, M. Saba, A critical review of asbestos concentrations in water and air, according to exposure sources, Heliyon 9 (2023), e15730.
[6] J. Curtius, M. Granzin, J. Schrod, Testing mobile air purifiers in a school classroom: reducing the airborne transmission risk for SARS-CoV-2, Aerosol Sci. Technol. 55 (2021) 586–599.
[7] D. Wang, B.-C. Sun, J.-X. Wang, Y.-Y. Zhou, Z.-W. Chen, Y. Fang, W.-H. Yue, S.-M. Liu, K.-Y. Liu, X.-F. Zeng, G.-W. Chu, J.-F. Chen, Can masks be reused after hot water decontamination during the COVID-19 pandemic? Engineering 6 (2020) 1115–1121.
[8] S. Choi, H. Jeon, M. Jang, H. Kim, G. Shin, J.M. Koo, M. Lee, H.K. Sung, Y. Eom, H.-S. Yang, J. Jegal, J. Park, D.X. Oh, S.Y. Hwang, Biodegradable, efficient, and breathable multi-use face mask filter, Adv. Sci. 8 (2021), 2003155.
[9] T. Lu, J. Cui, Q. Qu, Y. Wang, J. Zhang, R. Xiong, W. Ma, C. Huang, Multistructured electrospun nanofibers for air filtration: a review, ACS Appl. Mater. Interfaces 13 (2021) 23293–23313.
[10] M. Kaminski, J.M. Gac, P. Sobiech, P. Kozikowski, S. Jakubiak, T. Jankowski, Filtration of submicron soot particles, oil droplets, and their mixtures on single- and multi-layer fibrous filters, Aerosol Air Qual. Res. 22 (2022), 210258.
[11] Z. Wang, Z. Zhao, J. Baucom, D. Wang, L. Dai, J.-F. Chen, Nitrogen-doped graphene foam as a metal-free catalyst for reduction reactions under a high gravity field, Engineering 6 (2020) 680–687.
[12] D. Persaud, M. Smirnov, D. Fong, P. Sanaei, Modeling of the effects of pleat packing density and cartridge geometry on the performance of pleated membrane filters, Fluid 6 (2021) 209.
[13] S. Liu, Z. Lin, F. Xiao, J. Zhang, D. Wang, X. Chen, Y. Zhao, J. Xu, Co-N-C in porous carbon with enhanced lithium ion storage properties, Chem. Eng. J. 389 (2020), 124377.
[14] H. Wu, Q. Sun, J. Chen, G.-Y. Wang, D. Wang, X.-F. Zeng, J.-X. Wang, Citric acid-assisted ultrasmall CeO_2 nanoparticles for efficient photocatalytic degradation of glyphosate, Chem. Eng. J. 425 (2021), 130640.
[15] X. Xie, J. Shi, Y. Pu, Z. Wang, L.-L. Zhang, J.-X. Wang, D. Wang, Cellulose derived nitrogen and phosphorus co-doped carbon-based catalysts for catalytic reduction of p-nitrophenol, J. Colloid Interface Sci. 571 (2020) 100–108.
[16] S. Liu, F. Li, D. Wang, C. Huang, Y. Zhao, J.-B. Baek, J. Xu, 3D macroporous MoxC@N-C with incorporated Mo vacancies as anodes for high-performance lithium-ion batteries, Small Methods 2 (2018), 1800040.
[17] J. Leng, J. Chen, D. Wang, J.-X. Wang, Y. Pu, J.-F. Chen, Scalable preparation of Gd_2O_3:Yb^{3+}/Er^{3+} upconversion nanophosphors in a high-gravity rotating packed bed reactor for transparent upconversion luminescent films, Ind. Eng. Chem. Res. 56 (2017) 7977–7983.
[18] G.-H. Zhang, Q.-H. Zhu, L. Zhang, F. Yong, Z. Zhang, S.-L. Wang, Y. Wang, L. He, G.-H. Tao, High-performance particulate matter including nanoscale particle removal by a self-powered air filte, r. Nat. Commun. 11 (2020) 1653.
[19] W. Deng, Y. Sun, X. Yao, K. Subramanian, C. Ling, H. Wang, S.S. Chopra, B.B. Xu, J.-X. Wang, J.-F. Chen, D. Wang, H. Amancio, S. Pramana, R. Ye, S. Wang, Masks for COVID-19, Adv. Sci. 9 (2022), 2102189.
[20] S. Hu, H. Tian, S. Zhang, D. Wang, G. Gong, W. Yue, K. Liu, S. Hong, R. Wang, Q. Yuan, Y. Lu, D. Wang, L. Zhang, J. Chen, Fabrication of a high-performance and reusable planar face mask in response to the COVID-19 pandemic, Engineering 9 (2022) 101–110.
[21] Z. Feng, Z. Long, Modeling unsteady filtration performance of pleated filter, Aerosol Sci. Technol. 50 (2016) 626–637.
[22] Y.-L. Kim, M.-S. Kwon, M.-H. Lee, Optimized pleat geometry at specific pleat height in pleated filters for air purification, Indoor Air 32 (2022), e13135.
[23] J. Wang, D.R. Chen, D.Y.H. Pui, Modeling of filtration efficiency of nanoparticles in standard filter media, J. Nanoparticle Res. 9 (2007) 109–115.
[24] J. Wang, D.Y.H. Pui, Filtration of aerosol particles by elliptical fibers: a numerical study, J. Nanoparticle Res. 11 (2009) 185–196.
[25] J. Shi, Y. Zou, J.-X. Wang, X.-F. Zeng, G.-W. Chu, B.-C. Sun, D. Wang, J.-F. Chen, Investigation on designing meltblown fibers for the filtering layer of a mask by cross-scale simulations, Ind. Eng. Chem. Res. 60 (2021) 1962–1971.
[26] D.C. Freshwater, J.I.T. Stenhouse, The retention of large particles in fibrous filters, AIChE J. 18 (1972) 786–791.
[27] W.C. Hinds, Aerosol Technology: Properties, Behavior, and Measurement of Airborne Particles, third ed., John Wiley & Sons, New York, 2012.
[28] I.B. Stechkina, N. Fuchs, Studies on fibrous aerosol filters-I. Calculation of Diffusional deposition of aerosols in fibrous filters, Ann. Occup. Hyg. 9 (1966) 59–64.
[29] S. Kuwabara, The forces experienced by randomly distributed parallel circular cylinders or spheres in a viscous flow at small Reynolds numbers, J. Phys. Soc. Jpn. 14 (1959) 527–532.
[30] Z.G. Liu, P.K. Wang, Pressure drop and interception efficiency of multifiber filters, Aerosol Sci. Technol. 26 (1997) 313–325.
[31] T. Yu, Y.B. Zhao, Computational modeling of filtration efficiency of electret air filter media, J. Filtr. Sep. 27 (2017) 27–32.
[32] P. Zhao, P. Cheng, B.J. Tatarchuk, Loading of fibrous filter media and newly designed filter configurations by salt particles: an experimental study, AIChE J. 62 (2016) 3739–3750.
[33] D.-Q. Chang, S.-C. Chen, A.R. Fox, A.S. Viner, D.Y.H. Pui, Penetration of sub-50 nm nanoparticles through electret HVAC filters used in residence, Aerosol Sci. Technol. 49 (2015) 966–976.
[34] A.M. Saleh, H.V. Tafreshi, A simple semi-numerical model for designing pleated air filters under dust loading, Sep. Purif. Technol. 137 (2014) 94–108.
[35] C.R. Ethier, Flow through mixed fibrous porous materials, AIChE J. 37 (1991) 1227–1236.
[36] B. Cao, F. Qian, M. Ye, Y. Guo, S. Wang, J. Lu, Y. Han, Pressure drop model for fibrous media in depth filtration: coupling simulation of microstructure and CFD porous media during dust loading, Build. Environ. 202 (2021), 108015.